RESEARCH REPORTS
Biological

K. Musselmann[1]*, J.A. Green[1], K. Sone[1], J.C. Hsu[1], I.R. Bothwell[1], S.A. Johnson[1], J.S. Harunaga[1], Z. Wei[2], and K.M. Yamada[1]*

[1]Cell Biology Section, Laboratory of Cell and Developmental Biology, Division of Intramural Research, National Institute of Dental and Craniofacial Research, 30 Convent Drive, MSC 4370, Bethesda, MD 20892, USA; and [2]Developmental Mechanisms Section, Division of Intramural Research, National Institute of Dental and Craniofacial Research, 30 Convent Drive, MSC 4326, Bethesda, MD 20892, USA; *corresponding authors, kurt.musselmann@gmail.com and kenneth.yamada@nih.gov

J Dent Res 90(9):1078-1084, 2011

Salivary Gland Gene Expression Atlas Identifies a New Regulator of Branching Morphogenesis

ABSTRACT

During organ development, local changes in gene expression govern morphogenesis and cell fate. We have generated a microanatomical atlas of epithelial gene expression of embryonic salivary glands. The mouse submandibular salivary gland first appears as a single mass of epithelial cells surrounded by mesenchyme, and it undergoes rapid branching morphogenesis to form a complex secretory organ with acini connected to an extensive ductal system. Using laser capture microdissection, we collected samples from 14 distinct epithelial locations at embryonic days 12.5, 13.5, 14, and 15, and characterized their gene expression by microarray analysis. These microarray results were evaluated by qPCR of biological replicates and by comparisons of the gene expression dataset with published expression data. Using this gene expression atlas to search for novel regulators of branching morphogenesis, we found a substantial reduction in mRNA levels of GSK3β at the base of forming clefts. This unexpected finding was confirmed by immunostaining, and inhibition of GSK3β activity enhanced salivary gland branching. This first microanatomical expression atlas of a developing gland characterizes changes in local gene expression during salivary gland development and differentiation, which should facilitate the identification of key genes involved in tissue morphogenesis.

KEY WORDS: microarray, laser microdissection, branching morphogenesis, GSK3beta, organ morphogenesis, gene expression.

DOI: 10.1177/0022034511413131

Received December 16, 2010; Last revision May 13, 2011; Accepted May 13, 2011

A supplemental appendix to this article is published electronically only at http://jdr.sagepub.com/supplemental.

INTRODUCTION

The architecture of many epithelial organs is first established during embryonic development by the process of branching morphogenesis (Davies, 2006). During branching morphogenesis, a simple epithelial structure subdivides by budding, clefting, and/or invagination to form a more complex structure (Affolter *et al*., 2003; Hogan, 2006; Andrew and Ewald, 2010). Morphogenesis of the mouse salivary gland has been a classic experimental model for understanding this morphogenetic process for more than a half-century (Grobstein, 1953).

Development of the mouse submandibular salivary gland begins at embryonic day (E)11.5 and has been extensively described (Tucker, 2007). As the gland grows, clefts begin to form in the buds. These clefts deepen to define end buds and secondary ducts. By E13, the submandibular salivary gland has 3 to 4 secondary ducts leading into individual endbuds. These buds undergo further clefting events, which produce new endbuds and ducts. This process is repeated many times, generating the acinar structure of the mature gland.

The factors that initiate cleft formation are not yet known, although many interactions and signaling pathways influence the subsequent process of branching morphogenesis. Many growth factor signaling pathways (Patel *et al*., 2006) and extracellular matrix components (Spooner and Faubion, 1980; Hosokawa *et al*., 1999; Sakai *et al*., 2003; Rebustini *et al*., 2007) have been shown to be important for organogenesis of the salivary gland and other branching organs. Isolated mesenchyme-free epithelia can still undergo branching morphogenesis in the presence of appropriate growth factors and extracellular matrix (Morita and Nogawa, 1999; Larsen *et al*., 2006). Consequently, the epithelium contains all of the information needed for branching morphogenesis.

We describe here the generation of an atlas of gene expression at microanatomical resolution of the developing salivary gland using laser capture microdissection (LCM). We isolated mRNA from highly localized regions of salivary gland epithelia from 12.5-, 13.5-, 14-, and 15-day-old embryos and analyzed it using microarrays. Gene expression data for epithelial cells at forming clefts, peripheral and central buds, and main or secondary ducts were obtained and compared. This high-resolution spatiotemporal atlas should facilitate the discovery of novel markers, regulators, and mechanisms of early gland development, and serve as a source of new ideas for experimentally testable hypotheses.

We searched this database for a novel regulator of salivary gland cleft formation. By comparing gene expression in epithelial cells located at the

base of E13.5 clefts *vs*. cells in the neighboring peripheral bud, we found that mRNA levels of GSK3β appeared strikingly decreased at the base of the cleft compared with the rest of the bud. GSK3β is at the crossroads of cell adhesion signaling *via* cadherins, as well as WNT, FGF, and other growth factor signaling pathways (Espinosa *et al*., 2003; Katoh, 2006; Maher *et al*., 2009). We therefore investigated the role of GSK3β in salivary development by immunolocalization and inhibitor studies and identified GSK3β as a novel regulator of salivary gland branching morphogenesis.

MATERIALS & METHODS

Detailed descriptions of the methods used are provided in the Appendix.

Submandibular Gland (SMG) Culture

E11 timed-pregnant ICR strain mice were obtained from Harlan (Indianapolis, IN, USA). SMGs were cultured on 0.1-μm-pore Nuclepore filters (GE Healthcare, Piscataway, NJ, USA) as previously described (Larsen *et al*., 2006). E12 salivary glands were cultured until clefts were readily visible, but all other stages were frozen immediately after isolation. Frozen sectioning and laser capture microdissection were performed with a CM3050S cryostat (Leica Microsystems, Wetzlar, Germany) and an Arcturus^{XT} Microdissection System (Applied Biosystems, Carlsbad, CA, USA).

Microarray Analysis and qPCR Validation

RNA isolated from LCM samples was amplified twice with MessageAMP 2 AA (Ambion, Austin, TX, USA) and analyzed with Mouse Whole Genome Arrays (4x44k, Agilent, Santa Clara, CA, USA). Raw data were quantile-normalized (Bolstad *et al*., 2003) and analyzed with GeneSpring 11.5 (Agilent); gene expression was validated by qPCR. The data are available now in a searchable format at http://sgmap.nidcr.nih.gov and at GEO (Accession number GSE22828). Independent biological replicates (n = at least 3) were amplified once and analyzed by SYBR-Green qPCR in a StepOnePlus thermal cycler (Applied Biosystems) with ddCT used to calculate fold change.

GSK3β Inhibitory Studies

E12 SMGs were treated with GSK3β inhibitors 20 mM LiCl (Klein and Melton, 1996), 10 μM S3442 (SB-216763) (Cross *et al*., 2001), or 5 μM BIO (6-bromoindirubin-3′-oxime; Sigma-Aldrich, St. Louis, MO, USA) (Polychronopoulos *et al*., 2004) with appropriate vehicle controls.

Whole-mount and Cryosection Immunofluorescence Microscopy

SMGs were stained as previously described (Rebustini *et al*., 2007). Primary antibodies were E-cadherin (ECCD-2, Invitrogen, Carlsbad, CA, USA), GSK3β (Cell Signaling, Danvers, MA, USA), or custom rabbit polyclonal fibronectin antibody R5386; secondary antibodies were from Jackson ImmunoResearch Laboratories (West Grove, PA, USA).

Cryosections (14 μm) of E12 SMGs cultured until E13.5 were fixed with acetone-methanol and stained for 1 hr at RT. Samples were examined by confocal microscopy (LSM 510 or 710, Carl Zeiss, Oberkochen, Germany).

RESULTS

Chip Assessment, Validation, and Initial Bioinformatic Analysis

Epithelial cells from distinct locations of the developing salivary gland (Fig. 2A and Appendix Fig. 1), including the base of clefts, central and peripheral buds, and secondary and main ducts, were isolated by laser microdissection, and their gene expression was analyzed with microarrays. The first issue we addressed was whether the microarray data from independent biological replicates would cluster according to location and age. We performed hierarchical clustering analysis of arrays based on age or location and found that the biological replicates clustered closer to each other according to location or according to age (Figs. 1A, 1B and Appendix Fig. 2). The E12.5 and E13.5 bud arrays were similar to each other but different from the E14 and E15 arrays, which were also similar (Fig. 1A). The E13.5 and E14 secondary ducts had similar expression profiles, but the E15 secondary ducts were distinct (Appendix Fig. 2C). At each age studied, the main and secondary duct arrays were similar, and differed from the bud arrays (Appendix Figs. 2E-2G). In the E12.5 arrays, expression in the cleft and bud samples was more similar than that in the main duct samples (Fig. 1B). A dendrogram of all the arrays showed that the arrays group into 8 clusters (Appendix Fig. 3). The results of this clustering suggest that differences of gene expression between the isolated locations could be identified. However, the E13.5 peripheral and central bud arrays were nested, as were the main and secondary ducts at E13.5, E14, and E15, indicating that gene expression in these subsets of arrays was very similar.

We then assessed whether our data accurately reflected published records of gene expression in the developing SMG. We generated a list of genes recognized as markers of SMG during development that included the ductal markers *Fxyd2, Klk1, Krt7, Krt19*, *Scnn1b,* and *Tcfcp2l1* (Yamaguchi *et al*., 2006), a late endbud marker, *Aqp5* (Larsen *et al*., 2009), the SMG differentiation markers *Dcpp1, Dcpp2, Dcpp3, Smgc,* and *Pip*, and early SMG markers *Etv4, Fgfr2,* and *Mmp2* (Lombaert and Hoffman, 2010). The expression levels detected in our arrays clearly show spatiotemporal patterns that closely match the literature concerning these markers (Fig. 1C).

We selected 23 genes that exhibited differences in their microarray spatial or temporal expression pattern for further evaluation by qPCR, including 6 genes involved in Wnt signaling. In total, 29 qPCR comparisons were performed, and in 27 reactions the trends in the relative gene expression of the microarrays were confirmed (Table 1 and data not shown).

To identify functions or pathways of genes differentially expressed (≥ 10-fold) between buds and ducts, we uploaded the gene lists to DAVID (http://david.abcc.ncifcrf.gov/) (Huang da *et al*., 2009) for analysis. Elevated gene expression identified

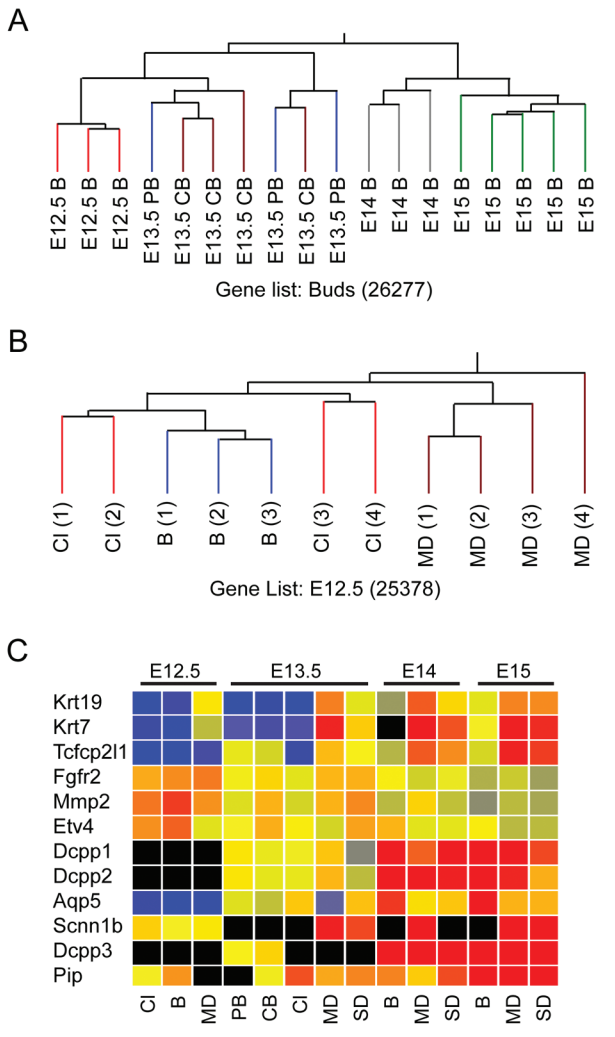

Figure 1. Chip and message level analysis of SGMAP arrays. Abbreviations for all panels: B – bud; Cl – cleft; MD – main duct; SD – secondary duct; PB – peripheral bud; CB – central bud. The numbers in parentheses indicate the total number of genes present or marginal in 2 out of 3 arrays. **(A)** Hierarchical clustering of bud arrays from ages E12.5 to E15. The arrays generally cluster according to age, with gene expression in E12.5 and E13.5 bud arrays more similar to each other, while the E14 and E15 bud arrays are highly similar to each other. **(B)** Hierarchical clustering of E12.5 arrays. All arrays are nested, and the bud and cleft arrays group closer to each other compared with the main duct arrays. **(C)** Normalized gene expression of markers of salivary gland development as quantified in SGMAP arrays. The genes cluster into 3 groups: In Group 1, Krt19, Krt7, and Tcfcp2l1 are ductal maturation markers; in Group 2, Fgfr2, Mmp2, and Etv4 are expressed mainly in initial bud and pseudoglandular stages (E12.5 and E13.5); and in Group 3, Dcpp -1,-2,-3 and Pip are markers for salivary gland maturation, and Aqp5 and Scnn1b are markers for terminal differentiation of SMG epithelial cells (acinar and duct, respectively). Fxyd2, Kik1, and SMGC were excluded by the software before the clustering because they were detected only in E15 arrays.

in the E15 duct included genes associated with the Wnt pathway and certain substrate-specific transporters, whereas genes up-regulated in the bud included enzyme activators and several non-categorized genes (Table 1 and Appendix Tables 1–3). A similar approach was used to compare buds at E12.5 *vs.* E15 at ≥ 15-fold differences in expression (because of the larger number of differentially expressed genes). Up-regulated gene classes included metallopeptidases in the E12.5 buds and peptidase inhibitors in the E15 buds (Table 1 and Appendix Tables 5, 6). Together, the clustering of the biological replicates, the spatio-temporal agreement of our data with published data, and qPCR validation demonstrate that our arrays accurately describe gene expression in the developing SMGs.

Post hoc Analysis

Although the cells of the cleft are part of the endbud (Fig. 2A), their arrays subcluster separately from the central and peripheral bud arrays (Fig. 2B). We found significant differences in gene expression between the cleft and other sites in the bud. The E13.5 dataset was filtered by ANOVA to identify statistically significant ($p < 0.05$) differential gene expression. We found that 3698 genes are significantly differently expressed at distinct locations at that age (out of 22,067 genes detected). After Tukey's *post hoc* analysis, 241 genes were identified with differential expression in cleft epithelial cells compared with the central bud (and 104 genes compared with the peripheral bud), as well as 1889 genes in the duct compared with the central bud. Similar analysis of the E14 and E15 arrays shows that more genes are expressed differently in the bud compared with the main duct than between the main duct compared with the secondary duct [Appendix Table 7; the differentially expressed genes identified by ANOVA plus Tukey's test have been deposited in GEO (GSE22828)]. These results suggest that although the arrays may appear similar by dendrogram analysis, differences in gene expression can be detected even when the locations are situated within micrometers of each other. Furthermore, analysis of our temporal data suggests that intrinsic expression differences between main and secondary ducts and bud *vs.* duct are maintained during development of the salivary gland.

Using the Atlas to Identify a Novel Candidate Regulator of Branching Morphogenesis

We searched for novel regulators of branching morphogenesis by comparing gene expression between the E13.5 bud and the cleft, and found that expression of *GSK3*β was significantly lower in the cleft (Fig. 2C). In addition, we examined E13.5 protein expression by staining for GSK3β. The staining was most prominent in the cells immediately adjacent to the basement membrane and decreased at the base of the cleft compared with the adjacent cells of the peripheral bud (2.4-fold lower protein intensity), mirroring the previously described decreased staining for E-cadherin (Fig. 2D) (Sakai *et al.*, 2003). GSK3β can affect E-cadherin stability (Lickert *et al.*, 2000); therefore, we hypothesized that a decrease in GSK3β activity might enhance cleft formation.

GSK3β Inhibition Affects Branching Morphogenesis

Treatment of E12 SMGs with 20 mM LiCl to inhibit GSK3β resulted in striking morphological changes in the glands (Fig. 3A). By 12 hrs, treated SMGs showed increased numbers

of deep clefts, though they did not extend further to form secondary ducts by 16 or 24 hrs. After 16 hrs of treatment, the control glands had an average of 3.5 clefts, whereas treated glands had 5.5, a 60% increase ($P < 0.0001$, n = 68) (Fig. 3B). These clefts showed fibronectin accumulation similar to that in untreated glands (Fig. 3C), and, upon removal of LiCl inhibition, progressed to form secondary ducts (Fig. 3D). LiCl also stimulated epithelial branching in mesenchyme-free epithelial rudiments embedded in laminin (Fig. 3E).

To confirm specificity for GSK3β, we repeated these experiments with 2 additional pharmacological inhibitors: SB-216763 and BIO. Treatment with SB-216763 significantly increased branching by 40 hrs (not shown). Particularly striking effects were observed with BIO. Treated salivary glands showed well-developed extra clefts 5 hrs after treatment (Fig. 3F); as with LiCl, these clefts did not progress to form secondary ducts. Together, these studies, prompted by unexpected data from the expression atlas, indicate that decreased GSK3β activity promotes the initiation of branching, though GSK3β activity is necessary later for successful formation of secondary ducts.

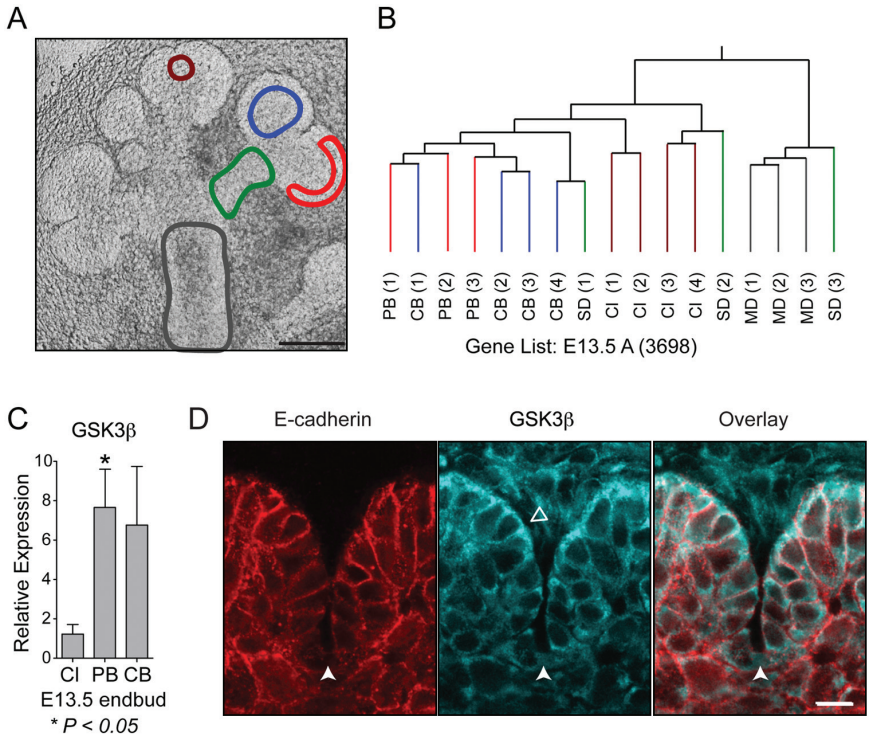

Figure 2. E13.5 ANOVA analysis, qPCR, and immunostaining for GSK3β. **(A)** A representative E13.5 salivary gland showing examples of the epithelial regions isolated by laser capture microdissection: peripheral bud (red), central bud (blue), cleft (brown), main duct (gray), and secondary duct (green). Scale bar = 100 μm. **(B)** Hierarchical clustering based on genes from E13.5 arrays passing ANOVA ($P < 0.05$) (indicated by the suffix A). The arrays cluster into separate groups containing the bud arrays, cleft arrays, or main duct arrays; the secondary duct arrays did not sort together. **(C)** qPCR confirmation of *GSK3β* levels in the bud compared with those in the cleft. *GSK3β* is expressed at significantly lower levels in the cleft compared with the peripheral bud ($P = 0.03$). **(D)** GSK3β immunostaining (aqua) of a 14-μm cryosection from an E13.5 salivary gland. E-cadherin (red) staining is found at all epithelial cell-cell junctions, with a decrease in intensity at the base of clefts. GSK3β is particularly prominent in the peripheral epithelial cells (open arrowhead) adjacent to the basement membrane. GSK3β levels are markedly decreased at the base of clefts (denoted by the white arrowhead). Scale bar = 10 μm.

DISCUSSION

Organ development requires spatially and temporally coordinated expression of multiple genes within specific subsets of cells. The purpose of this study was to describe and validate a new spatial gene expression database for use by the research community for discovering novel, site-specific regulators and mechanisms of branching morphogenesis of mammalian salivary glands. This characterization of the microanatomical epithelial transcriptome of the submandibular salivary gland reveals major differences in patterns of gene expression at different regions at early stages of gland morphogenesis. This information should accelerate future research by providing a resource for generating new hypotheses about the regulation and mechanisms of morphogenesis.

Our preliminary bioinformatic analyses identified location- and stage-specific differential expression of a variety of interesting genes, pathways, and sets of functions. Availability of the primary dataset should invite further bioinformatic analyses to identify new markers for each location within the developing gland. Validation and functional analyses of sets of unique and common regulatory genes should provide a better understanding of organ branching and differentiation.

Several genes locally up-regulated in epithelial cells immediately adjacent to forming clefts and necessary for branching morphogenesis of salivary glands and lungs have previously been described (Onodera *et al*., 2010). We used the dataset described here to search for the opposite type of regulation: a potential regulatory gene that is down-regulated in the cells that form clefts. Expression of GSK3β was markedly reduced in cells at the base of forming clefts. Our experimental analysis revealed that transient loss of GSK3β activity promotes the initial formation of clefts. Besides the gene expression patterns, these conclusions are based on the similar effects of 3 different GSK3β inhibitors tested, all of which stimulated cleft formation. Moreover, experiments with epithelial rudiments lacking any mesenchyme indicated that the effects are due solely to inhibitory action on the epithelium and not secondary effects of mesenchymal inhibition. Furthermore, the extra clefts formed with GSK3β inhibition display the local accumulation of fibronectin that characterizes natural clefts. After release from inhibition, natural and inhibitor-induced clefts all mature to form the deep

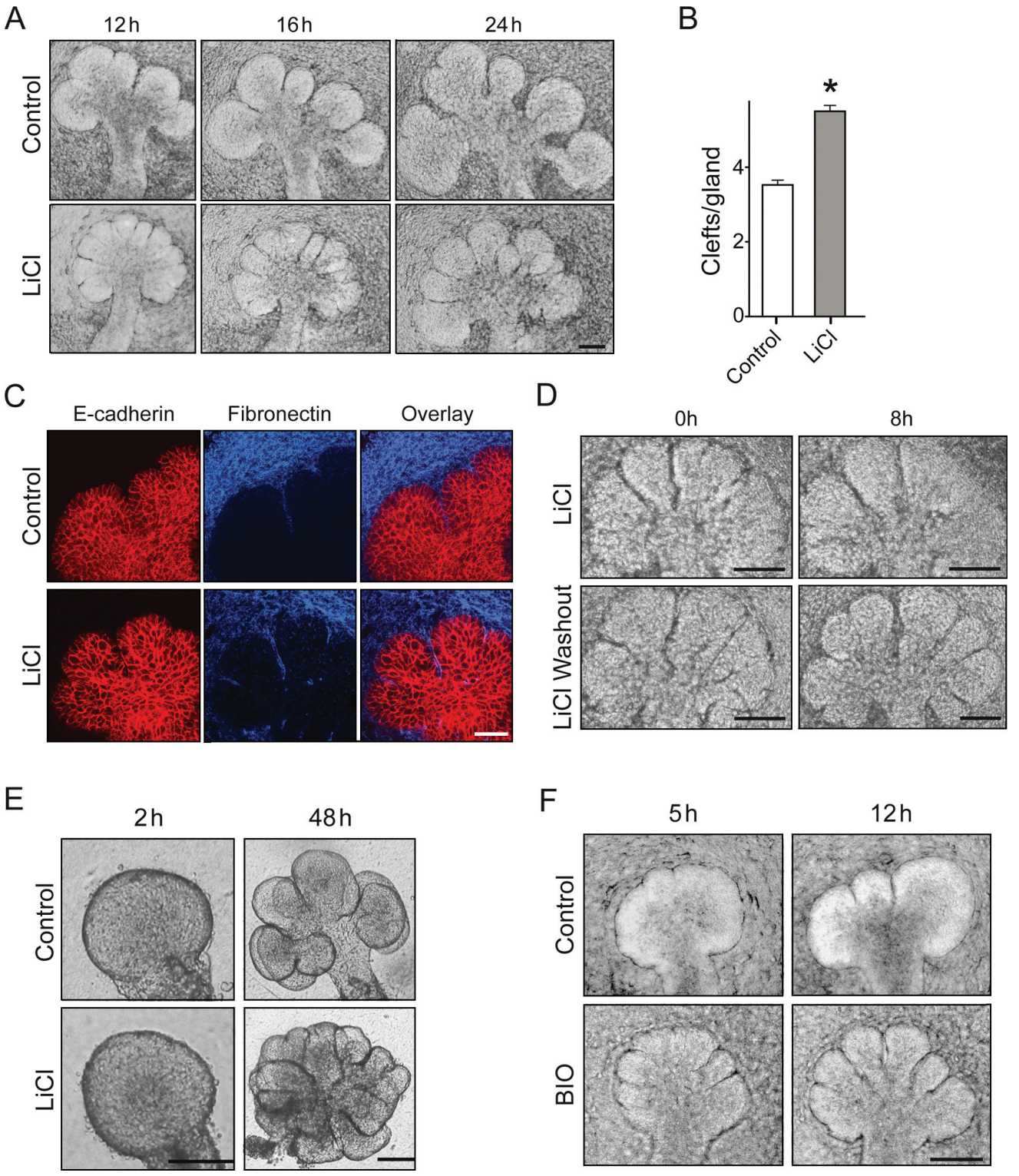

Figure 3. Effect of GSK3β inhibition on salivary gland branching morphogenesis. E12.5 salivary glands were used for all experiments. **(A)** Salivary gland morphology after culture in 20 mM NaCl (control) or 20 mM LiCl. LiCl-treated glands show an increase in the number of clefts at 12 and 16 hrs, but the glands at 16 and 24 hrs show inhibition of secondary duct formation. **(B)** Quantification of clefts/gland after 16 hrs in LiCl, *one-tailed *t* test, $p < 0.0001$ ($n = 68$). **(C)** Staining of treated salivary glands for E-cadherin (red) and fibronectin (blue). Clefts show fibronectin accumulation in the NaCl control (top panels) and LiCl-treated glands (lower panels). **(D)** Salivary gland morphology after LiCl removal (top panels) or continued LiCl treatment (lower panels). The time after removal of the inhibitor is indicated (t = 0 after 16 hrs of LiCl treatment); removal of the GSK3β inhibitor permits secondary duct formation to proceed. **(E)** Isolated mesenchyme-free epithelial rudiment cultured in medium supplemented with 20 mM LiCl also demonstrates stimulated branching. **(F)** Treatment with 5 μM BIO shows extra clefts forming by 5 hrs after start of treatment, but the clefts fail to mature into secondary ducts.

Table 1. Embryonic Day 15 Bud *vs.* Main Duct, Selected Functions, and Pathways of Genes Differentially Expressed

Gene Symbol	Fold Change in Microarray	Fold Change by qPCR	References with Localization Data
Adherens junction/Tight junction/Cell adhesion/Focal Adhesion			
Cdh1	−1.5	−4.6	–
Cldn10	a	–	**IF: E17 bud**; Appendix Ref.1
Cldn11	b	–	**IF: E16 duct**; Appendix Ref.1
Cldn4	−7.4	–	**IF: E16 duct**; Appendix Ref.1
Egfr	−4.3	c	**IF: ducts**; Appendix Ref.2
Cldn6	b	–	**IF: E16 duct**; Appendix Ref.1
Itga6	1.2	1.5	**IF: epithelium**; Appendix Ref.3
Krt17	−3.7	−11	–
Krt18	−1.8	−3.5	**IF: epithelium**; Appendix Ref. 4
Krt19	−5	–	**ISH: ducts**; Appendix Ref. 5
Krt7	−17	−66	**ISH: ducts**; Appendix Ref. 5
Krt8	−1.4	−1.7	**IF: epithelium**; Appendix Ref. 4
Lamb3	−16.9	−16.7	–
Substrate Specific Channel Activity			
Kcnn4	49	–	**IF: late bud**; Appendix Ref. 6, 7, 8
Aqp5	28	–	**qPCR: late bud**; Appendix Ref. 9, 10
Cftr	−9.2	–	**IF: ducts**; Appendix Ref. 11, 12
Scnn1a	−20.5	c	–
Scnn1b	−25	–	**ISH: E16 duct**; Appendix Ref. 5
Wnt signaling pathway			
Wnt10a	−155	−941	–
Wnt6	−2.5	−56.4	–
Ctnnb1#	−2.3	0	–
Non-categorized genes			
Dcpp1	84	9	**ISH: E14.5**; Appendix Ref. 13, 14
Dcpp2	92	20	**ISH: E14.5**; Appendix Ref. 13, 14
Dcpp3	52	8	**ISH: E14.5**; Appendix Ref. 13, 14
Enzyme activator activity			
Acap3	5.3	–	–
Gpsm3	20.5	–	–
Sec14l2	10.6	–	–
Mgst2	6.5	–	–
Rap1gap	6.6	–	–
Transcription factor activity			
Runx2	−6.1	–	–
Jun	−7.8	–	–
Creb5	−31.2	–	–
Dach1	−11.5	–	–
Mafb	−15.3	–	–
Meis2	−15	–	–

Key: –, no expression data at either the appropriate age or location available for that gene; #, qPCR data disagree with microarray results; a - no expression detected in duct arrays; b - no expression detected in bud arrays; c - not detected in bud samples; d - no expression detected in E12.5 bud; qPCR - localization by qPCR; IF - localization by immunofluorescence; ISH - localization by *in situ* hybridization.

clefts that eventually define secondary ducts. GSK3β is part of the canonical Wnt pathway, which has roles in the morphogenesis of some branching organs (Lin *et al*., 2001; De Langhe *et al*., 2005; Wang *et al*., 2008). Although Wnt signaling contributes to *Drosophila* salivary gland development (Harris and Beckendorf, 2007), it is not yet known to be involved in mammalian salivary gland development. In our dataset, we detected localized Wnt expression at all ages, suggesting that a role for Wnts in salivary development should be examined.

Analysis of these data, taken together, indicates that loss of GSK3β by either normal local transcriptional down-regulation or experimental pharmacological inhibition promotes the initiation of cleft formation, but that GSK3β activity must be restored for initial clefts to mature and delineate buds and secondary ducts. These findings identify GSK3β as a novel regulator of branching morphogenesis.

In summary, we have generated an atlas of gene expression at specific locations of a developing gland undergoing branching

morphogenesis. The dataset has been validated *in silico* compared with the published literature and by qPCR. Furthermore, analysis of the gene expression data led to the surprising identification of the involvement of GSK3β down-regulation in initiating endbud clefting. This dataset is part of the Salivary Gland Molecular Atlas Project of the NIDCR and has been made available for unrestricted use by the scientific community.

ACKNOWLEDGMENT

This work was supported by the Division of Intramural Research, National Institute of Dental and Craniofacial Research, National Institutes of Health (Bethesda, MD, USA). The authors declare no potential conflicts of interest with respect to the authorship and/or publication of this article.

REFERENCES

Affolter M, Bellusci S, Itoh N, Shilo B, Thiery JP, Werb Z (2003). Tube or not tube: remodeling epithelial tissues by branching morphogenesis. *Dev Cell* 4:11-18.

Andrew DJ, Ewald AJ (2010). Morphogenesis of epithelial tubes: insights into tube formation, elongation, and elaboration. *Dev Biol* 341:34-55.

Bolstad BM, Irizarry RA, Astrand M, Speed TP (2003). A comparison of normalization methods for high density oligonucleotide array data based on variance and bias. *Bioinformatics* 19:185-193.

Cross DA, Culbert AA, Chalmers KA, Facci L, Skaper SD, Reith AD (2001). Selective small-molecule inhibitors of glycogen synthase kinase-3 activity protect primary neurones from death. *J Neurochem* 77:94-102.

Davies JA, editor (2006). *Branching morphogenesis (Molecular Biology Intelligence Unit)*. New York: Springer Science.

De Langhe SP, Sala FG, Del Moral PM, Fairbanks TJ, Yamada KM, Warburton D, *et al*. (2005). Dickkopf-1 (DKK1) reveals that fibronectin is a major target of Wnt signaling in branching morphogenesis of the mouse embryonic lung. *Dev Biol* 277:316-331.

Espinosa L, Ingles-Esteve J, Aguilera C, Bigas A (2003). Phosphorylation by glycogen synthase kinase-3 beta down-regulates Notch activity, a link for Notch and Wnt pathways. *J Biol Chem* 278:32227-32235.

Grobstein C (1953). Inductive epitheliomesenchymal interaction in cultured organ rudiments of the mouse. *Science* 118:52-55.

Harris KE, Beckendorf SK (2007). Different Wnt signals act through the Frizzled and RYK receptors during *Drosophila* salivary gland migration. *Development* 134:2017-2025.

Hogan BL (2006). Building organs from buds, branches and tubes. *Differentiation* 74:323-325.

Hosokawa Y, Takahashi Y, Kadoya Y, Yamashina S, Nomizu M, Yamada Y, *et al*. (1999). Significant role of laminin-1 in branching morphogenesis of mouse salivary epithelium cultured in basement membrane matrix. *Dev Growth Differ* 41:207-216.

Huang da W, Sherman BT, Lempicki RA (2009). Systematic and integrative analysis of large gene lists using DAVID bioinformatics resources. *Nat Protoc* 4:44-57.

Katoh M (2006). Cross-talk of WNT and FGF signaling pathways at GSK3beta to regulate beta-catenin and SNAIL signaling cascades. *Cancer Biol Ther* 5:1059-1064.

Klein PS, Melton DA (1996). A molecular mechanism for the effect of lithium on development. *Proc Natl Acad Sci USA* 93:8455-8459.

Larsen HS, Ruus AK, Galtung HK (2009). Aquaporin expression patterns in the developing mouse salivary gland. *Eur J Oral Sci* 117:655-662.

Larsen M, Wei C, Yamada KM (2006). Cell and fibronectin dynamics during branching morphogenesis. *J Cell Sci* 119(Pt 16):3376-3384.

Lickert H, Bauer A, Kemler R, Stappert J (2000). Casein kinase II phosphorylation of E-cadherin increases E-cadherin/beta-catenin interaction and strengthens cell-cell adhesion. *J Biol Chem* 275:5090-5095.

Lin Y, Liu A, Zhang S, Ruusunen T, Kreidberg JA, Peltoketo H, *et al.* (2001). Induction of ureter branching as a response to Wnt-2b signaling during early kidney organogenesis. *Dev Dyn* 222:26-39.

Lombaert IM, Hoffman MP (2010). Epithelial stem/progenitor cells in the embryonic mouse submandibular gland. *Front Oral Biol* 14:90-106.

Maher MT, Flozak AS, Stocker AM, Chenn A, Gottardi CJ (2009). Activity of the beta-catenin phosphodestruction complex at cell-cell contacts is enhanced by cadherin-based adhesion. *J Cell Biol* 186:219-228.

Morita K, Nogawa H (1999). EGF-dependent lobule formation and FGF7-dependent stalk elongation in branching morphogenesis of mouse salivary epithelium in vitro. *Dev Dyn* 215:148-154.

Onodera T, Sakai T, Hsu JC, Matsumoto K, Chiorini JA, Yamada KM, (2010). Btbd7 regulates epithelial cell dynamics and branching morphogenesis. *Science* 329:562-565.

Patel VN, Rebustini IT, Hoffman MP (2006). Salivary gland branching morphogenesis. *Differentiation* 74:349-364.

Polychronopoulos P, Magiatis P, Skaltsounis AL, Myrianthopoulos V, Mikros E, Tarricone A, *et al*. (2004). Structural basis for the synthesis of indirubins as potent and selective inhibitors of glycogen synthase kinase-3 and cyclin-dependent kinases. *J Med Chem* 47:935-946.

Rebustini IT, Patel VN, Stewart JS, Layvey A, Georges-Labouesse E, Miner JH, *et al.* (2007). Laminin alpha5 is necessary for submandibular gland epithelial morphogenesis and influences FGFR expression through beta1 integrin signaling. *Dev Biol* 308:15-29.

Sakai T, Larsen M, Yamada KM (2003). Fibronectin requirement in branching morphogenesis. *Nature* 423:876-881.

Spooner BS, Faubion JM (1980). Collagen involvement in branching morphogenesis of embryonic lung and salivary gland. *Dev Biol* 77:84-102.

Tucker AS (2007). Salivary gland development. *Semin Cell Dev Biol* 18:237-244.

Wang BE, Wang XD, Ernst JA, Polakis P, Gao WQ (2008). Regulation of epithelial branching morphogenesis and cancer cell growth of the prostate by Wnt signaling. *PLoS One* 3:e2186.

Yamaguchi Y, Yonemura S, Takada S (2006). Grainyhead-related transcription factor is required for duct maturation in the salivary gland and the kidney of the mouse. *Development* 133:4737-4748.